# MULTIPATH EXPLOITATION WITH ADAPTIVE WAVEFORM DESIGN FOR TRACKING IN URBAN TERRAIN

*B. Chakraborty, Y. Li, J. J. Zhang, T. Trueblood, A. Papandreou-Suppappola, and* †*D. Morrell*

SenSIP Center, School of ECEE, Arizona State University, Tempe, AZ
†Department of Engineering, Polytechnic Campus, Mesa, AZ

**ABSTRACT**

We integrate multipath exploitation with adaptive waveform design in order to increase the tracking performance of a vehicle moving in urban terrain. Mitigation of both clutter and strong multipath returns can result in increased target detection. However, exploiting multiple bounces from obstacles such as buildings can be shown to increase radar coverage and scene visibility, especially in the absence of direct line-of-sight paths. For this purpose, we formulate the multipath propagation of an arbitrary number of specular bounces in urban terrain for three-dimensional motion. We then further exploit and optimize multipath returns by dynamically selecting the parameters of the transmitted waveform to minimize the predicted mean-squared tracking error. We demonstrate our proposed approach in a realistic urban environment by varying the type of measurement to include regions of obscuration and different number of multipath bounces.

***Index Terms***— Urban terrain, multipath exploitation, waveform-agile sensing, particle filtering, tracking.

## 1. INTRODUCTION

When operating in an urban environment, most radar systems could fail due to lack of line-of-sign (LOS) returns, interference from multipath signal reflections, and large and inconsistent returns (or clutter) from objects such as buildings [1]. Two major issues of urban radar is complete obscuration or shadowing (no received measurements) and multipath returns from signal reflections off surfaces that can result in varied range measurements and contradict LOS measurements. There are various techniques to overcome these problems. For example, either more sensors or airborne radar systems with very steep grazing angles can be used to combat obscuration. Also, multipath returns can be treated as interference and mitigated [2, 3]. However, there are scenarios in the urban environment where the direct path is lost, and the only paths available are the indirect multipaths. In such cases, by utilizing prior knowledge about the environment, such as road maps and building locations, multipath returns can be used to confirm the target detection proposed by the LOS measurements [4]. More recently, researchers have been studying multipath propagation [5], realizing the potential benefits of extracting target information from multipath returns to enhance tracking performance. An overview of the approaches that can be employed for tracking in an urban environment are presented in [6]. Especially when no LOS is available, multipath returns allow the detection and tracking of a target without LOS, thereby decreasing the obscuration effects from buildings and increasing the visible area in the urban environment [1]. This exploitation of information is thus expected to increase radar coverage and scene visibility.

The work was partly supported by MURI Grant AFOSR FA9550-05-1-0443 and by Lockheed Martin SenSIP Consortium Project 019950-005.

In this paper, we first formulate the multipath propagation geometry in urban terrain for an arbitrary number of specular bounces in three-dimensional (3-D) space. Using this geometry, we aim to further improve tracking performance by integrating waveform-agile sensing with multipath exploitation radar (WASMER). Specifically, we use a particle filter (PF) tracker for a single-target tracking scenario in a partially-obscured urban environment with different areas of sight. The PF incorporates nonlinear measurements and two different types of motion models to allow the target to move straight or turn. Assuming perfect detection, the agile sensing algorithm selects the parameters of the waveform to be transmitted at the next time step by minimizing the predicted tracking error covariance.

The paper is organized as follows. In Section 2, we derive the 3-D multipath geometry, and Sections 3 and 4 formulate the tracking with multipath exploitation and waveform optimization, respectively. Simulation results in Section 5 demonstrate the effectiveness of the joint WASMER system.

## 2. MULTIPATH PROPAGATION GEOMETRY IN 3-D

In [5], the 2-D multipath geometry from a radar to a target is derived under certain conditions for the path to exist. In this paper, we want to derive the multipath geometry in 3-D space and in terms of the possible multiple bounces that affect the target tracking estimation. Specifically, we consider a tracking problem where a transceiver radar located in 3-D space is transmitting a signal $s_T(t)$ in urban terrain. We assume that the signal is bouncing between two buildings such that it reflects off $M$ surfaces from the transmitter to the target, then it reflects off its intended target, and finally it reflect off $M'$, possibly different, surfaces from the target to the receiver. Our aim is to formulate the resulting 3-D multipath propagation geometry, assuming specular reflections (i.e., for the reflected rays, the angle of incidence equals the angle of reflection). We define a path to be the time it takes to travel between the radar and the target. Due to the specular assumption, if there are multiple bounces, a path would correspond to the time it takes to travel between the radar and a virtual target. A virtual target corresponds to a target with a fictional range and range rate that the LOS would have resulted in if the building was not obstructing the signal transmission.

Figure 1 illustrates an urban terrain for a radar located at location $(x_R, y_R, z_R)$ (in 3-D Cartesian coordinates). At time step $k$, the location and velocity of the target are given by $(x_k, y_k, z_k)$ and $(\dot{x}_k, \dot{y}_k, \dot{z}_k)$, respectively. In the figure, we only demonstrate LOS and one-bounce reflections. Specifically, only three possible paths are demonstrated: radar-to-target (LOS), radar-Building 1-target (one-bounce), and radar-Building 2-target (one-bounce). Each of the one-bounce paths have corresponding virtual targets, as demonstrated in Fig. 1. The range of the direct signal path at time $k$ is given by the Euclidean distance between the radar and the

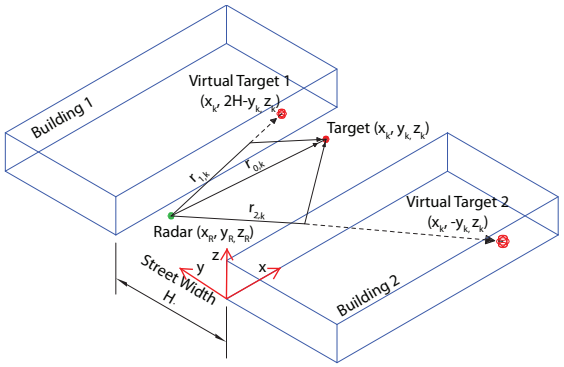


**Fig. 1**. Geometry of LOS and one-bounce multipath reflections.

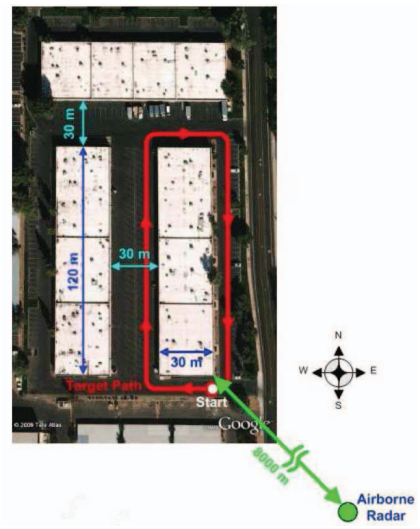


**Fig. 2**. Representative urban terrain, DARPA MER Program [7].

target: $r_{k,0} = ((x_k - x_R)^2 + (y_k - y_R)^2 + (z_k - z_R)^2)^{1/2}$. The range-rate is the derivative of range with respect to time: $\dot{r}_{k,0} = (\dot{x}_k(x_k - x_R) + \dot{y}_k(y_k - y_R) + \dot{z}_k(z_k - z_R))/r_{k,0}$. For simplicity, we consider the multipath geometry from the radar to the target; this can be symmetrically extended from the target to the radar. The range from the radar to the target after $m$ bounces is

$$r_{k,m,i} = \Big((x_k - x_R)^2 \tag{1}$$
$$+ \left[(-1)^{m+1}\left(2\left[\frac{m}{2}\right]_i H - (-1)^{i+1} y_k\right) - y_R\right]^2 + (z_k - z_R)^2\Big)$$

where $H$ is the street width. It is assumed that the first bounce was off Building $i$, $i = 1, 2$, where $[\frac{m}{2}]_1 = \lceil \frac{m}{2} \rceil$ and $[\frac{m}{2}]_2 = \lfloor \frac{m}{2} \rfloor$. The corresponding range-rate can be obtained by taking the derivative of the range in (1) with respect to time. In Fig. 1, $m = 1$, so there could be $P = 9$ possible paths after a round trip, and accordingly, the range and range-rate for the round trip are the summation of the range and range rate in each direction. When $m = 2$, the total number of paths would be $P = 25$ since two-bounce paths would be possible. Note, however, that real-data examples have shown that two-bounce reflections suffer from severe fading and are too weak to observe [7].

## 3. MULTIMODEL TRACKING WITH MULTIPATH

### 3.1. Representative Urban Terrain Example

Throughout the paper, we make use of an urban scene that was considered a representative example of a challenging urban environment by the Defense Advanced Research Projects Agency (DARPA) in their 2009 Multipath Exploitation Radar (MER) program [1]. This scene is depicted in Fig. 2 to consist of three buildings with a ground vehicle driving through urban terrain, following a loop trajectory. An airborne radar is located approximately $8,000$ m southeast of the scene and $1,400$ m high, resulting in a shallow grazing angle that prevents LOS when the target is traveling between the buildings. Using prior knowledge on the urban environment, we can determine different types of measurements in different areas. The map in Fig. 3 illustrates the available measurements for the different areas (indicated by different shaded regions), assuming perfect detection. The loop indicates the vehicle trajectory.

### 3.2. State-Space Formulation

In order to formulate the state space formulation for estimating the position and velocity of the ground vehicle ($z_k = 0$) in the urban terrain, consider the target state vector $\mathbf{X}_k = [x_k\ \dot{x}_k\ y_k\ \dot{y}_k]^T$ at time step $k$ and the measurement vector $\mathbf{Z}_k = [r_k\ \dot{r}_k]^T$, where $r_k$ and $\dot{r}_k$ are the range and range-rate measurements, respectively, and $T$ denotes vector transpose. The state process model is governed by two possible models, depending on whether the ground vehicle moves at a constant velocity or is turning. When moving at a constant velocity, the state transition is given by

$$\mathbf{X}_k = F\mathbf{X}_{k-1} + \mathbf{W}_k,$$

where $F$ is a $4 \times 4$ matrix such that, for example, $x_k = x_{k-1} + \dot{x}_{k-1}\delta t$ and $\dot{x}_k = \dot{x}_{k-1}$ [8], where $\delta t$ is the time interval between successive measurements. When the target is turning with a constant turning rate $\omega$, then $F$ is given by [9]

$$F = \begin{bmatrix} 1 & \sin(\omega\delta t)/\omega & 0 & -(1-\cos(\omega\delta t))/\omega \\ 0 & \cos(\omega\delta t) & 0 & -\sin(\omega\delta t) \\ 0 & (1-\cos(\omega\delta t))/\omega & 1 & \sin(\omega\delta t)/\omega \\ 0 & \sin(\omega\delta t) & 0 & \cos(\omega\delta t) \end{bmatrix}.$$

The measurement model is given by $\mathbf{Z}_k = \mathbf{h}_k(\mathbf{X}_k) + \mathbf{V}_k$, where $\mathbf{h}_k$ is a nonlinear function and $\mathbf{V}_k$ is additive Gaussian measurement noise with covariance $\mathbf{R}_k$. As the number of possible bounces can affect the number of paths, and due to multiple possible multipaths, we define the noise-free measurement $\mathbf{h}_k(\mathbf{X}_k)$ at time $k$ as

$$\mathbf{h}_k(\mathbf{X}_k) = \begin{bmatrix} r_{k,1} & r_{k,2} & \cdots & r_{k,P_k} \\ \dot{r}_{k,1} & \dot{r}_{k,2} & \cdots & \dot{r}_{k,P_k} \end{bmatrix},$$

where $r_{k,p}$ and $\dot{r}_{k,p}$ are the range and range rate measurements of the $p$th path at time step $k$, $p = 1, \cdots, P_k$, and $P_k$ is the total number of paths at time step $k$, which depends on the location of the target at that time.

### 3.3. Particle Filter Tracker

Particle filtering is used as the tracker due to the nonlinearity in the measurement model. As there are two possible types of motion, the process model must adaptively choose the type of motion at each time step using the multiple-model particle filter (MMPF) [10]. Using the MMPF, a model parameter needs to be estimated at each

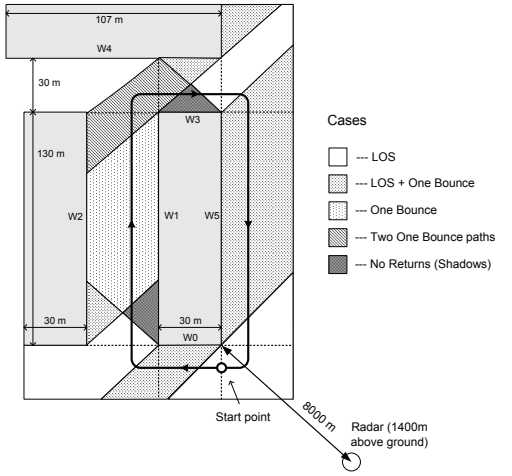


**Fig. 3**. Available measurement map for the simulated urban terrain.

time step based on the model at the previous time step and the preset transitional probability matrix $\Pi$ whose element $\pi_{ij}$ represents the transitional probability from model $i$ to model $j$. The MMPF automatically chooses the motion model and estimates the state at each time step $\mathbf{X}_k$ using the PF and the measurement $\mathbf{Z}_k$.

## 4. DYNAMIC WAVEFORM SELECTION

### 4.1. Signal and noise models

The waveform selection is designed to choose the parameters of the transmission signal in order to minimize the tracking estimation mean-squared error (MSE). The transmission signal considered is a Gaussian enveloped linear frequency-modulated (LFM) chirp, $s_T(t) = a(t)\, e^{j2\pi \frac{B}{T_d} t^2}$, where the Gaussian window is $a(t) = \left(\frac{1}{\pi\lambda^2}\right)^{1/4} e^{-t^2/(2\lambda^2)}$, $\lambda$ parameterizes the pulse length, and $B$ is the bandwidth of the signal. The effective pulse length $T_d$ is the time interval over which the signal amplitude is greater than $0.1\%$ of its maximum value. This criteria determines $\lambda = T_d/7.4338$ [11]. The unit normalized transmission signal with carrier frequency $f_c$ is then represented by $s(t) = \sqrt{2}\mathrm{Re}\left[s_T(t)e^{j2\pi f_c\, t}\right]$. For a ground vehicle moving in the urban terrain with $P$ multipath returns, the received signal is given by

$$s_r(t) = \sum_{p=1}^{P} \sqrt{2}\,\mathrm{Re}\Big\{\beta_p s_T(t-\tau_p)e^{j2\pi(f_c t+\nu_p t)}\Big\}, \qquad (2)$$

where $\beta_p$ is the reflection coefficient and $\tau_p$ and $\nu_p$ are the delay and Doppler shift components of the $p$th path. The received signal, $s_R(t) = s_r(t) + w(t)$, has a zero-mean additive white Gaussian noise (WGN) component $w(t)$. The radar measures the delay and Doppler related to the tracker range ($r_p$) and range-rate ($\dot{r}_p$) observations as $r_p = c\tau_p/2$ and $\dot{r}_p = c\nu_p/(2f_c)$ where $c$ is the speed of propagation of the transmitted signal. The error in the measurement of the delay and Doppler hence impacts the accuracy of the range and range rate observations.

The detection and estimation is performed in each range cell, and using the urban map, the total number of multipath returns can be calculated. Let the delay and Doppler parameters to be estimated be defined as $\Phi = [\phi_1\ \phi_2 \cdots\ \phi_p]^T$ where $\phi_p = [\tau_p\ \nu_p]$. Using this discretization, the received signal can be expressed as $s_R[n] = s_r[n;\Phi] + w[n]$, where $w[n]$ are independent zero-mean WGN samples with variance $\sigma^2$. The estimation of $\Phi$ is equivalent to estimating a vector signal parameter in the presence of WGN. The Fisher information matrix (FIM) for estimating $\Phi$ is given by [12]

$$[\mathbf{I}(\Phi)]_{ij} = \frac{1}{\sigma^2}\sum_{n=1}^{N} \frac{\partial s_r[n;\Phi]}{\partial \phi_i}\frac{\partial s_r[n;\Phi]}{\partial \phi_j} \qquad (3)$$

and $\mathrm{CRLB}(\Phi) = \mathbf{I}(\Phi)^{-1}$ corresponds to the Cramér-Rao lower bound (CRLB) for the delay and Doppler estimate variance. From (3), the CRLB depends on the transmission waveform parameters. Let $\boldsymbol{\theta}_k = [\lambda_k\ B_k]^T$ represent the waveform parameter vector which describes the LFM chirp. The noise covariance for the measurement of range and range-rate is therefore a function of the waveform parameters and found by $\mathbf{R}(\boldsymbol{\theta}_k) = \boldsymbol{\Gamma}\,\mathbf{I}(\Phi)^{-1}\,\boldsymbol{\Gamma}^T$, where $\boldsymbol{\Gamma}$ is a diagonal matrix with $P$ block diagonal matrices, $\boldsymbol{\gamma}_p = \mathrm{diag}(c/2,\ c/(2f_c)), p = 1, \cdots\ P_k$.

### 4.2. Cost function computation

We consider a library of $L$ waveform parameter vectors, $\boldsymbol{\theta}^l$, $l = 1, \cdots, L$. At every time step $k$, we seek to choose the parameter in the library which minimizes the tracking MSE $\mathbf{J}(\boldsymbol{\theta}_k)$. The trace of the state covariance matrix $\mathbf{P}_{k|k}(\boldsymbol{\theta}_k)$ can be used to approximate $\mathbf{J}(\boldsymbol{\theta}_k)$. This covariance matrix can be computed using the Kalman filter covariance update equation for linear measurement models. For nonlinear measurement models, an approximate solution for the Kalman filter covariance update can be found using the unscented transform (UT) [13]:

$$\hat{\mathbf{P}}_{k|k}(\boldsymbol{\theta}_k) = \mathbf{P}_{k|k-1} - \mathbf{P}_{XZ}(\mathbf{P}_{ZZ} + \mathbf{R}(\boldsymbol{\theta}_k))^{-1}\mathbf{P}_{XZ}^T. \qquad (4)$$

The estimated state error covariance for each of the $l$ waveforms in the library is thus given by,

$$\hat{\mathbf{P}}_{k|k}(\boldsymbol{\theta}_k^l) = \mathbf{P}_{k|k-1} - \mathbf{P}_{XZ}(\mathbf{P}_{ZZ} + \mathbf{R}(\boldsymbol{\theta}_k^l))^{-1}\mathbf{P}_{XZ}^T$$

We evaluate the cost function $\mathbf{J}(\boldsymbol{\theta}_k^l) = \mathrm{trace}(\hat{\mathbf{P}}_{k|k}(\boldsymbol{\theta}_k^l))$ at every time step for the entire library of waveforms and choose that $\boldsymbol{\theta}_l$ which provides the minimum $\mathbf{J}(\boldsymbol{\theta}_k)$.

## 5. SIMULATIONS

We simulate tracking with dynamic waveform selection using the urban terrain example in Section 3.1. The single ground moving target is assumed to be moving at a speed of 5 m/s. A library of constant time-bandwidth product and unit energy signals was created with 0.1 $\mu$s minimum and 1 ms maximum pulse durations. The bandwidth was chosen to be between 1 kHz to 10 MHz. The carrier frequency was $f_c = 1$ GHz and the velocity of propagation of the waveform was $c = 3 \times 10^8$ m/s. The measurements were simulated such that there was a loss of 10 dB in energy for every reflection. At every time step, waveforms are chosen from a library so as to minimize the cost function in Section 4.2. The true target trajectory and the estimated target trajectory obtained using the waveform selection algorithm are shown in Fig. 4. The performance deterioration in the shadow regions is expected as there are no measurements received during that time; the state vector is only updated by the process model. The selected waveform duration and bandwidth parameters at every time step are shown in Fig. 5.

We compare the performance of the tracking system using waveform selection with an open loop system which transmits waveforms

from the library in a round-robin fashion. The comparison of the MSE in tracking the position and velocity in both the systems is shown in Fig. 6 and Fig. 7. Except for the shadow regions, we can observe the reduced MSE performance achieved with waveform-agile tracking.

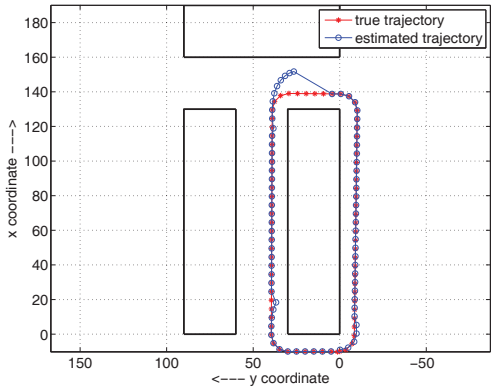


**Fig. 4**. True and estimated target trajectory.

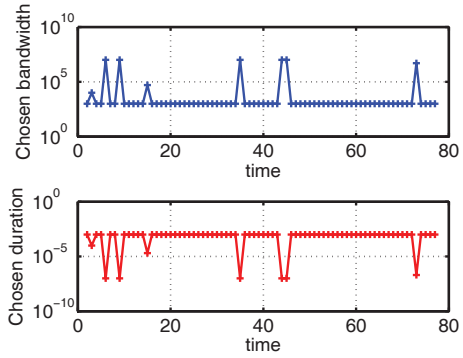


**Fig. 5**. Waveform parameter selection.

## 6. CONCLUSION

We considered the problem of dynamic waveform design for tracking a ground moving vehicle in an urban environment. We formulated multipath geometry in 3-D space, and then we integrated multipath exploitation with waveform design to increase target tracking performance. Application of the proposed approach to a challenging urban scene demonstrated the decrease in mean-squared estimation error.

## 7. REFERENCES


[1] J. Durek, "Multipath exploitation radar industry day presentation," 2009, www.darpa.mil/STO/solicitations/baa09-01/presentations/MER_Industry_Day.pdf.


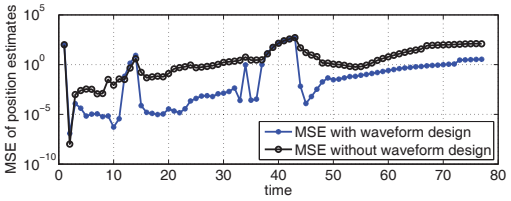


**Fig. 6**. Averaged MSE of position estimates.

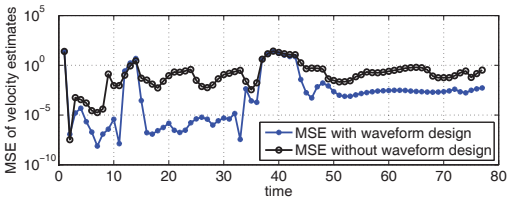


**Fig. 7**. Averaged MSE of velocity estimates.


[2] B. Krach and R. Weigel, "Markovian channel modeling for multipath mitigation in navigation receivers," in *European Conf. Antennas and Propagation*, March 2009, pp. 1441–1445.

[3] B. D. Rigling, "Urban RF multipath mitigation," *IET Radar, Sonar and Navigation*, vol. 2, pp. 419–425, December 2008.

[4] M. Mertens and M. Ulmke, "Precision GMTI tracking using road constraints with visibility information and a refined sensor model," in *IEEE Radar Conference*, May 2008, pp. 1–6.

[5] J. L. Krolik, J. Farrell, and A. Steinhardt, "Exploiting multipath propagation for GMTI in urban environments," in *IEEE Conference on Radar*, April 2006, pp. 65–68.

[6] P. R. Barbosa, E. K. P. Chong, S. Suvarova, and B. Moran, "Multitarget-multisensor tracking in an urban environment: A closed-loop approach," in *Proc. SPIE: Int. Society for Optical Engineering*, 2008, vol. 6969.

[7] "MER data collection review," www.darpa.mil/STO/solicitations/baa09-01/presentations/MER_Data_Review.pdf.

[8] T. Trueblood, "Multipath exploitation radar for tracking in urban terrain," M.S. thesis, Arizona State University, 2009.

[9] X. R. Li and V. P. Jilkov, "Survey of maneuvering target tracking. Part I. Dynamic models," *IEEE Transactions on Aerospace and Electronic Systems*, vol. 39, pp. 1333–1364, October 2003.

[10] B. Ristic, S. Arulampalam, and N. Gordon, *Beyond the Kalman filter: Particle filters for tracking applications*, Artech House, 2004.

[11] D.J. Kershaw and R.J Evans, "Optimal waveform selection for tracking systems," *IEEE Transactions on Information Theory*, vol. 40, pp. 1536–1550, September 1994.

[12] S. M. Kay, *Fundamentals of Statistical Processing, Volume I: Estimation Theory*, Prentice Hall, 1993.

[13] S. P. Sira, A. Papandreou-Suppappola, and D. Morrell, "Dynamic configuration of time-varying waveforms for agile sensing and tracking in clutter," *IEEE Transactions on Signal Processing*, vol. 55, pp. 3207–3217, July 2007.